

Dopplerons and the Gantmakher-Kaner effect in a compensated-metal plate

I. F. Voloshin, V. G. Skobov, L. M. Fisher, and A. S. Chernov

V. I. Lenin All-Union Electrotechnical Institute

(Submitted 21 July 1981)

Zh. Eksp. Teor. Fiz. **82**, 293–309 (January 1982)

The dependence of the impedance of a compensated-metal plate on a magnetic field H perpendicular to the plate is investigated theoretically and experimentally. The calculation was performed for a model in which the hole Fermi surface has the shape of a corrugated cylinder, and the electrons are local. The dependences of the smooth part of the impedance, of the doppleron-oscillation amplitude, and of the Gantmakher-Kaner oscillations (GKO) on the magnetic field are obtained for the two circular polarizations of the exciting field, assuming diffuse reflection of the carriers. The calculation results agree with the experimental data. The nonlocal Fisher-Kao effect is observed in thin specimens. The behavior of the GKO amplitudes is found to differ qualitatively in thin and in thick films. It is shown that the substantial difference between the GKO amplitudes for the different circular polarizations, observed in the vicinity of the doppleron threshold, is due to the diffuse reflection of the carriers.

PACS numbers: 72.15.Eb

The surface impedance of a metal plate in a perpendicular magnetic field has been the subject of many studies. The first theoretical calculations were performed under the assumption of specular reflection of the carriers from the metal surface. It turned out in this case that the impedance of a semi-infinite metal has a resonant maximum at the doppleron threshold ($H = H_L$), and it is determined above the threshold completely by the normal skin effect in the magnetic field. It was shown in addition that the oscillating part of the plate impedance, due to the Gantmakher-Kaner effect, does not depend on the sign of the circular polarization of the radio-frequency field. The results of experiments performed on a number of metals have shown that the behavior of the smooth part of the impedance does not follow the rules predicted by the theory. In particular, a kink rather than a maximum of the impedance is observed at the doppleron threshold. The oscillating parts of the impedance also behave differently in experiment and in the theory. Thus, in the theory the amplitude of the doppleron oscillations decreases with increasing magnetic field much more rapidly than in experiment. In addition, in the field region $H < H_L$ a strong difference was observed between the amplitudes of the Gantmakher-Kaner oscillations (GKO) in the two circular polarizations.

These discrepancies have stimulated the development of a theory for the case of diffuse reflection of carriers. It was demonstrated first that in this theory the impedance of a semi-infinite metal does indeed have a kink at the doppleron threshold. Since the calculation of the plate impedance under diffuse reflection, in the general formulation of the problem, is extremely complicated, a simple lucid theory was developed, which is valid in strong fields $H \gg H_L$. It turned out that nonlocal effects alter radically the character of the skin effect under diffuse-reflection conditions. This theory, however, is not valid for moderate and weak magnetic fields, where many singularities appear in the observed phenomena: a doppleron threshold, a maximum of the doppleron oscillations, and a difference between the GKO in the cir-

cular polarizations.

We have previously¹ developed a more general method of solving the problem of the plate impedance, in which its behavior can be investigated in the entire range of fields.¹⁾ In the present paper we calculated by this method the smooth and oscillating parts of the plate impedance for the corrugated-cylinder model and show, in particular, that in the doppleron-threshold region the amplitudes of the GKO in the two circular polarizations can differ greatly. The impedance of tungsten and molybdenum plates was measured and the results of the theory and experiment compared.

1. CALCULATION OF IMPEDANCE

1. We consider a compensated-metal model in which the hole part of the Fermi surface (FS) is in the form of a corrugated cylinder, while the electron part is a right circular cylinder.² The axes of both cylinders are parallel to the normal to the plate and to the constant magnetic field H , whose direction we align with the z axis. In this case the nonlocal conductivity for circular polarizations of the field is of the form

$$\sigma_{\pm}(q) = \pm i \frac{Nec}{H} s_{\pm}(q) = \mp i \frac{Nec}{H} \{ [(1 \mp i\gamma)^2 - q^2]^{-1/2} - (1 \mp i\gamma) \}, \quad (1)$$

$$q = \frac{k u}{2\pi}, \quad u = \frac{c}{eH} \left(\frac{\partial S}{\partial p_{\pm}} \right)_{\max}, \quad \gamma = \frac{u}{2\pi l}, \quad (2)$$

where k is the wave vector, N and l are the concentration and mean free path of the holes, $S(p_{\pm})$ is the area of the intersection of their FS with the plane $p_{\pm} = \text{const}$, u is the maximum displacement of the holes during the cyclotron period, and γ_1 is the ratio of the electron-collision frequency to their cyclotron frequency. We shall consider hereafter the magnetic-field region where $\gamma \ll 1$ and $\gamma_1 \ll 1$.

The first term in the curly brackets of (1) describes the Doppler-shifted cyclotron resonance (DSCR) of the holes, and the second describes the local conductivity of the electrons. Since a parallel exposition for the two polarizations can lead to confusion, we obtain first the

results for positive and then for negative polarization.

The dispersion equation for the field in an unbounded metal is of the form

$$D(q) = q^2 - \xi_0 s(q) = 0, \quad \xi_0 = \omega Ne u^2 / \pi c H. \quad (3)$$

This equation can be extended over the entire two-sheet Riemann surface. It then becomes equivalent to a bi-cubic equation, whose solutions p_n can be represented with the aid of the relations

$$p_{n+1} = \Gamma^2 y_n; \quad (4)$$

$$y_n = 1 - \frac{2}{3} t + \frac{i}{3} \left[\exp\left(-\frac{2\pi i n}{3} + \frac{K}{3}\right) - t^2 \exp\left(\frac{2\pi i n}{3} - \frac{K}{3}\right) \right]; \quad n=0, 1, 2;$$

$$K = \ln \left\{ \left[t^6 - \left(t^3 - \frac{27}{2} \xi_0^3 \right)^2 \right]^{1/2} + i \left(t^3 - \frac{27}{2} \xi_0^3 \right) \right\}; \quad (5)$$

$$t = 1 - \xi_1, \quad \xi_1 = \xi \Gamma \Gamma_1, \quad \xi = \xi_0 / \Gamma^3, \quad \Gamma = -1 + i\gamma, \quad \Gamma_1 = -1 + i\gamma_1. \quad (6)$$

In (5), the "square root" function is defined on the first sheet with a cut along the negative real axis. The six roots are disposed pairwise symmetrically about the origin. We shall designate by p_1 , p_2 , and p_3 the roots located in the upper half-planes of both sheets of the Riemann surface of the function D , with p_1 and p_2 located on the first sheet, and p_3 on the second. In the region of strong magnetic fields, where $\xi_0 \ll 1$, the root p_2 is close to -1 and corresponds to a doppleron, while the root p_1 is small and corresponds to the skin component of the field. In the vicinity of the doppleron threshold ($\xi = 2$), p_1 and p_2 are of the same order. Below the threshold ($\xi_0 > 2$) the root p_2 becomes small and p_1 large and almost pure imaginary. In this field region, p_2 corresponds to the skin component of the field, and p_1 to a "damped helicon" due to the local conductivity of the electrons. To describe the skin component in the entire field region by a root having the same designation, we introduce new definitions:

$$q_1 = \begin{cases} p_2 & \xi_0 > 2 \\ p_1 & \xi_0 < 2 \end{cases}, \quad q_2 = \begin{cases} p_1 & \xi_0 > 2 \\ p_2 & \xi_0 < 2 \end{cases}, \quad q_3 = p_3. \quad (7)$$

General expressions for the plate impedance Z under antisymmetrical excitation were obtained earlier.¹ It was shown that they become much simpler when the oscillations are relatively small and, in addition, the Fisher and Kao effect³ takes place in a field that exceeds H_L noticeably. We shall assume these conditions to be satisfied. Substituting the function $D(q)$ in Eqs. (12), (13), and (15) from Ref. 1 and carrying out the transformations described in the Appendix, we represent the expression for the impedance in the form

$$Z = R - iX = Z_1 - \frac{c}{8\pi q_0} Z_1^2 [2c_0^2 g_{sp}(L) + b_0^2 D'(q_2) e^{i q_2 L}]; \quad (8)$$

$$\frac{8\pi q_0}{c Z_1} = \frac{4\pi q_0}{c Z_\infty} + a_0^2 D'(q_1) e^{i q_1 L} \left[1 - \frac{a_0^2}{2q_1} D'(q_1) e^{i q_1 L} \right]; \quad (9)$$

$$\frac{4\pi q_0}{c Z_\infty} = q_1 + q_2 - \frac{1}{2} \Gamma - \frac{1}{\pi} \left[q_1 \arcsin \frac{q_1}{\Gamma} + q_2 \arcsin \frac{q_2}{\Gamma} - q_3 \arcsin \frac{q_3}{\Gamma} \right]; \quad (10)$$

$$a_0 = -\frac{2q_1(q_1 + q_2)}{D'(q_1)} e^{i(q_1)}, \quad b_0 = -\frac{2q_2(q_1 + q_2)}{D'(q_2)} e^{i(q_2)},$$

$$c_0 = -1/2 (q_1 + \Gamma)(q_2 + \Gamma_1) e^{i(\Gamma)}, \quad D'(q) = dD(q)/dq; \quad (11)$$

$$I(q) = -\frac{1}{2} \ln \left(1 + \frac{q}{\Gamma} \right) + \frac{\xi}{\pi} \int_0^{\infty} \frac{(3z^2 + 1 - \xi_1) \ln[(1+z^2)^{1/2} + q\Gamma^{-1}]}{(1+z^2)[(z^2 - \xi_1)^2 + z^2] + \xi^2 - \xi_1^2} dz; \quad (12)$$

$$g_{sp}(L) = \frac{2\xi}{\pi\Gamma} e^{i\Gamma L} \int_0^{\infty} \frac{z^2 \exp[i\Gamma L((1+z^2)^{1/2} - 1)]}{(1+z^2)[(z^2 - \xi_1)^2 + z^2] + \xi^2 - \xi_1^2} \frac{dz}{(1+z^2)^{1/2}}, \quad (13)$$

where $q_0 = \omega u / 2\pi c$, $L = 2\pi d / u$, $\omega = 2\pi f$ is the field frequency, d is the plate thickness, and Z_∞ is the impedance of the semi-infinite metal.

The smooth part of the plate impedance is determined with the first term of (8), i.e., by Z_1 . The quantity q_1 in (10) and the second term in (9) represent the contribution of the skin component of the field, and the presence of the second term in (9) may not be necessarily large compared with the damping depth of the skin component. The term q_2 in (10) is connected with excitation of the doppleron in the metal, and the remaining terms in (10), while expressed in terms of q_1 , q_2 , and q_3 , constitute the contribution of the integral along the edges of the cut (see A.4), i.e., they are connected with the excitation of the Gantmakher-Kaner component (GKC). The second term in (8) represents the oscillating part of the plate impedance. The term proportional to $\exp(iq_2 L)$ is due to the penetration of the doppleron through the plate, while the term with $g_{sp}(L)$ is due to the GKC. It is appropriate to mention here that in the case of specular reflection of the carriers the impedance oscillating part connected with the GKC is equal to $(8\pi q_0 / c) \cdot 2g_{sp}(L)$.

We consider now the cases in which Eq. (8)–(13) become noticeably simpler. The integral (13) can be calculated at large and small values of $L\xi_0^2$. Neglecting small terms proportional to γ , we have

$$g_{sp}(L) = 2\xi_0 (2\pi L)^{-1/2} \exp\left[-\gamma L - i\left(L + \frac{\pi}{4}\right)\right] \times \begin{cases} (L\xi_0^2)^{-1} \exp(-\pi i/2), & L\xi_0^2 \gg 1 \\ 1, & L\xi_0^2 \ll 1 \end{cases} \quad (14)$$

In the region of strong magnetic fields, where $\xi_0 \ll 1$, the right-hand side of (10) is equal to $\xi/\pi + q_1$; in addition¹

$$-a_0^2 D'(q_1) / 2q_1 \approx 1, \quad c_0 = 1/2, \quad b_0^2 D'(q_2) \approx \xi_0^2.$$

As a result, the expressions for the impedance take the form

$$Z = Z_1 - \frac{c}{8\pi q_0} Z_1^2 \left[\frac{1}{2} g_{sp}(L) + \xi_0^2 e^{i q_2 L} \right], \quad (15)$$

$$Z_1 = \frac{8\pi q_0}{c} \left(\frac{\xi_0}{\pi} + q_1 \frac{1 + e^{i q_1 L}}{1 - e^{i q_1 L}} \right)^{-1}, \quad (16)$$

$$q_1 = [i(\gamma + \gamma_1)\xi_0]^{1/2}, \quad q_2 = -1 + \frac{1}{2} \xi_0^2 + i\gamma. \quad (17)$$

The behavior of the impedance in strong fields was investigated earlier.^{2,4,5} However, since different parts of (15) and (16) were contained in Ref. 2 and 5, while the equations of Ref. 4 contain errors, we have presented the complete equation for Z . An expression for the smooth part of the plate impedance, similar to (16), was first given by Zherebchevskii and Naberezhnykh.⁴ A later paper by the same authors,⁶ however, devoted to a comparison of (16) with experi-

ment, contains an incorrect interpretation of this equation. It is stated that (16) describes the contribution of the normal skin effect in the entire field region where $q_1 \ll 1$, while the contributions connected with doppleron excitation in the GKC "should be small by virtue of the smallness of the wavelength compared with the skin thickness." Actually, Eq. (16) is valid in the field region $\xi_0 \ll 1$. In addition, the normal skin effect is defined as the situation wherein all the components of the field can be neglected compared with the skin component. Although at $\xi_0 \ll 1$ the electric field of the skin component is much stronger than the remaining components, the magnetic field may turn out to be also weaker. It is precisely the term ξ_0/π which characterizes the magnetic field of the GKC. Therefore the normal skin effect sets in only in very strong fields when these terms can be neglected ($\xi_0 \ll \gamma$ for thick plates $d \gg l$; $\xi_0 L \ll 1$ for thin ones). In weaker fields, (but still with $\xi_0 \ll 1$) the GKC magnetic field predominate and therefore the screening of the field in the metal (the skin effect) is determined simultaneously by the skin component and by the GKC.

In the field region $\xi_0 \sim 1$, all three components (skin, doppleron, and GKC) participate in the screening of the field. Unfortunately, in this field region the integral (12) cannot be expressed in terms of elementary functions.

In weak fields, when $\xi_0 \sim 1$, the amplitudes of both the skin components and the GKC turn out to be small on the metal surface and the screening of the field in the metal is determined by a damped helicon ($q_0 \approx i\xi_0^{1/2}$). Neglecting the terms that contain γ , calculating the integrals in (12), and simplifying (9) and (10), we obtain for the impedance the expression

$$Z = \frac{8\pi q_0}{c} \left\{ \left[i\xi_0^{1/2} + \frac{1}{2\pi} \ln(4\xi_0) \right]^{-1} - \frac{1}{4} e^{-2\eta} g_{sp}(L) \right\}, \quad (18)$$

$$\eta = \frac{1}{\pi} \int_0^{\infty} \ln[1 + (1+x^2)^{-1/2}] \frac{dx}{1+x^2} \approx 0.58.$$

It follows from (18) that in this field region the GKO amplitudes for diffuse and specular reflection differ by a factor $(1/8) \exp(-2\eta) \approx 0.039$.

We present analogous expressions for the minus polarization. The solutions of the dispersion equation are given by

$$q_{n+1}^3 = \Gamma^2 y_n; \quad (19)$$

$$y_n = 1 - 2^{1/2} i^{1/2} \{ \exp[2^{1/2} \pi i (n-2) + 1/2 K] - t^2 \exp[-2^{1/2} \pi i (n-2) - 1/2 K] \};$$

$$n=0, 1, 2,$$

$$K = \ln \{ \ln[-i(t^2 - (t^2 - 27/2 \xi_0^2)^{1/2})]^{1/2} + i(t^2 - 27/2 \xi_0^2)^{1/2} \}; \quad (20)$$

$$t = 1 - \xi_0, \quad \xi_1 = \xi \Gamma \Gamma_1, \quad \xi_2 = \xi_0 / \Gamma^2, \quad \Gamma = 1 + i\gamma, \quad \Gamma_1 = 1 + i\gamma_1. \quad (21)$$

As before, the roots q_1 , q_2 , and q_3 are those lying in the upper half planes, with q_2 and q_3 on the second sheet and the root q_1 , which characterizes the skin component, on the first sheet. The doppleron root turns out to be on the second sheet in accordance with the fact that there is no doppleron in this polarization. The factor $-i$ in the equation for K is introduced under the square-root sign to ensure that the roots of the dispersion equation do not fall on the cut of the "square

root" function.

The expressions for the plate impedance are obtained with the aid of transformations similar to those used in the derivation of (8)–(13). The final result is obtained from (8)–(13) in which the quantities Γ , Γ_1 , ξ , and ξ_1 are replaced by new ones in accordance with (21), b_0 in (8) is set equal to zero, and Eqs. (10) and (11) are replaced by

$$\frac{8\pi q_0}{cZ_{\infty}^{(-)}} = q_1 - \frac{1}{2} \Gamma - \frac{1}{\pi} \left\{ q_1 \arcsin \frac{q_1}{\Gamma} - q_2 \arcsin \frac{q_2}{\Gamma} - q_3 \arcsin \frac{q_3}{\Gamma} \right\}, \quad (22)$$

$$a_0^{(-)} = 2q_1 [D'(q_1)]^{-1} \exp[I(q_1)], \quad c_0^{(-)} = (1/2) (q_1 + \Gamma) \exp[I(\Gamma)]. \quad (23)$$

From now on we shall designate the polarization by the index $(-)$. The asymptotic expression for the function $g_{sp}^{(-)}$ at large and small values of $L\xi_0^2$ are obtained from (14) by complex conjugation. The expression for the plate impedance $Z^{(-)}$ in strong fields differs from (15) in that the second term in the square brackets, which is connected with the doppleron, is missing and that $g_{sp}^{(+)}$ is replaced by $g_{sp}^{(-)}$ ($q_1^{(-)} = q_1^{(+)}$ in this field region).

In the weak fields, the roots $q_{2,3} = \pm \xi_0^{1/2} + i$, which are located on the second sheet, turn out to be close to the cuts and in the distribution of the field in the metal it is possible to separate three components: skin component, GKC, and the components connected with the roots $q_{2,3}$, which we shall call a quasihelicon. Just as for the plus polarization, the amplitudes of the skin component and of the GKC turn out to be small, and the smooth part of the impedance is determined by the quasihelicon. The expression for the total impedance is

$$Z^{(-)} = \frac{8\pi q_0}{c} \left(\xi_0^{-1/2} - \frac{1}{4} e^{-2\eta} g_{sp}^{(-)}(L) \right). \quad (24)$$

We note that the asymptotic forms (18) and (24) for weak fields, just as Eqs. (8)–(13), can be used only so long as the electrons can be regarded as local. In addition, in calculating the asymptotic forms we have neglected the quantities γ and γ_1 , assuming that $\gamma = \gamma_1 = 0$, but these quantities increase with decreasing field.

2. Equations (15) and (16) can explain the behavior of the GKO amplitude $g(H)$ in string fields $\xi_0 \ll 1$. In specular carrier reflection, the GKO amplitude, increasing like $H^{1/2}$, reaches a maximum in a field $L\xi_0^2 \sim 1$, and then decreases like $H^{-9/2}$. The position of the maximum with respect to the magnetic field H_{GK}^{sp} varies with the plate thickness like $H_{GK}^{sp} \propto d^{1/5}$. In the case of diffuse reflection, the behavior of the GKO is entirely different, since an important role is assumed by the factor $|cZ_1/8\pi q_0|^2$. The factor q_0^{-2} is proportional to H^2 , while $|Z_1|^2$ increases monotonically in the region $\xi_0 \ll 1$ and reaches saturation in fields exceeding the value H_m at which the surface resistance $R_1(H)$ of the plate has a maximum. If $H_m > H_{GK}^{sp}$ (we assume hereafter this condition to be satisfied), the maximum of the GKO amplitude may turn out to occur in a field H_{GK} much stronger than H_{GK}^{sp} .

In what follows we need to know the value of H_m as a

function of the plate thickness d and of the average carrier mean free path $l_0 = u/\pi(\gamma + \gamma_1)$. We express the function $R_1(H)$ in the form

$$R_1(x) = \frac{8\pi\omega d}{c^2 x} \left(\beta x + \frac{\text{sh } x - \sin x}{\text{ch } x - \cos x} \right) \left[\left(\beta x + \frac{\text{sh } x - \sin x}{\text{ch } x - \cos x} \right)^2 + \left(\frac{\text{sh } x + \sin x}{\text{ch } x - \cos x} \right)^2 \right]^{-1/2}, \quad (25)$$

$$\beta = \frac{a}{b} \frac{l_0}{d}, \quad x = \left(\frac{2\pi b d^2}{u_L l_0} \right)^{1/2} \frac{H_L}{H}; \quad (26)$$

where u_L is the value of u at $H = H_L$.

We have used here in place of (16) and (17) a more general expression valid for a model with arbitrary resonant singularity of the nonlocal conductivity; a and b are numerical coefficients that depend on the FS model. The coefficient a is defined by Eq. (12) of Ref. 5, and b is defined as

$$s(q) = i(\gamma + \gamma_1) + q^2/b + \dots, \quad (27)$$

which is the expansion of the function $s(q)$ in powers of q^2 . It follows from (27) and (3) that $\xi_0 = b(H_L/H)^3$. For the corrugated-cylinder model $a = 2/\pi$ and $b = 2$. Differentiating (25) with respect to the magnetic field and equating the derivative to zero, we obtain an equation for $H_m(d, l_0, H_L)$. Since the equation contains combinations of the quantity l_0 , d , and H_L , it is useful to find a universal function $x_m(\beta)$, where x_m is the position of the maximum of the function $R_1(x)$. Curve 1 of Fig. 1 is a plot of the function $(\beta x_m)^{-1}$ against β^{-1} . The choice of the coordinate scales becomes clear from an analysis of (26). This plot illustrates the dependence of H_m on the thickness d at fixed values of l_0 and H_L . At the same time, by using this plot it is possible to plot H_m as a function of l_0 at fixed d .

The expression for the field H_m in the limiting cases of strong ($d \ll l_0$) and weak ($d \gg l_0$) spatial dispersion were obtained by us earlier.⁵ Although Eqs. (21) and (22) of Ref. 5 give the correct dependence of H_m on d and l_0 , we made errors in the coefficients [this pertains also to the intermediate formulas (14)–(20)]. The expressions for H_m should be

$$H_m = \left(\frac{2\pi b d^2}{l_0 u_L} \right)^{1/2} H_L \left(\frac{\beta + 1/3}{2} \right)^{1/2} = d^{1/2} \left[\frac{2H_L^3}{\Delta H d} \left(1 + \frac{\pi d}{3l_0} \right) \right]^{1/2}, \quad l_0 \gg d, \quad (28)$$

$$H_m = \left(\frac{2\pi b d^2}{l_0 u_L} \right)^{1/2} H_L \frac{1 + \beta}{2.254} = d \frac{2\pi^{1/2}}{2.254} \left(\frac{H_L^3}{l_0 \Delta H d} \right)^{1/2} \left(1 + \frac{l_0}{\pi d} \right), \quad l_0 \ll d. \quad (29)$$

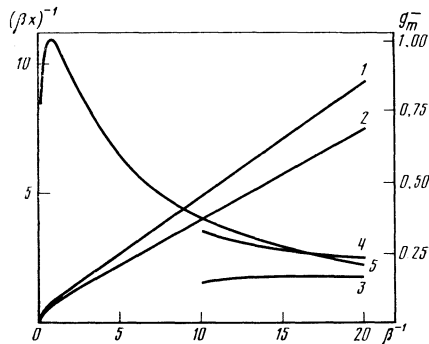


FIG. 1. Positions of the maxima of $R_1(H)$ and of the amplitude of the GKO (curves 1–3, left-hand scale) and of the maximum GKO amplitude (curves 4 and 5, right-hand scale).

In the second parts of the equations we have expressed u_L in terms of the period ΔH of the GKO, namely $u_L = \Delta H d / H_L$ (the product $\Delta H d$ does not depend on d), and substituted the numerical values of the constants a and b for our model. In (29) we have retained the second term of the expansion in the parameter l_0/d . While this term is small, it plays an essential role. It demonstrates that the asymptote ($d \rightarrow \infty$) of the $H_m(d)$ curve does not go through the origin, and it intercepts on the ordinate axis is

$$\delta H_m = \frac{a}{2.254} \left(\frac{2\pi l_0 H_L^3}{b \Delta H d} \right)^{1/2} = \frac{2}{2.254\pi^{1/2}} \left(\frac{l_0 H_L^3}{\Delta H d} \right)^{1/2}. \quad (30)$$

We note also that addition of the number $1/3$ to β under the square root in (28) makes it possible to use (28) also in the region $\beta \sim 1$. Moreover, it turns out that allowance for the next terms is inessential down to $\beta \sim 0.2$, when Eqs. (28) and (29) become joined within 3%.

To find the maximum of the function $g(H)$ we rewrite it in the field region $H > H_{GK}^D$, using (15)–(17) and the lower expression of (14), in the notation of (26):

$$e^{s/1} g = \frac{2^3 \omega u_L^3 l_0^{3/2}}{\pi^3 c^2 d} x^{3/2} \left[\left(\beta x + \frac{\text{sh } x - \sin x}{\text{ch } x - \cos x} \right)^2 + \left(\frac{\text{sh } x + \sin x}{\text{ch } x - \cos x} \right)^2 \right]^{-1/2}. \quad (31)$$

We have separated here the exponential decrease of the oscillations, due to the finite mean free path l . We note that in the case when the conductivity has a singularity of a different type it is necessary to replace (14) by the appropriate expression for g_{sp} . As a result, the function g will be described by an equation similar to (31), in the numerator of which it is necessary to change the degree of the quantity x and the numerical factor. Let us find the position x_{GK} of the maximum of the function g . For small thicknesses ($\beta \gg 1$) we usually obtain

$$x_{GK} = (3/2)^{1/2} x_m = (3/2)^{1/2} [2/(\beta + 1/3)]^{1/2}. \quad (32)$$

Thus, the GKO turn out to have a maximum in a field only 14% weaker than $H_m(d)$, and varies in proportion with it with increasing plate thickness. Starting with a certain value of d ($\beta = 0.1$), the situation is changed. In addition to the maximum, which varies as before with the maximum of the function $R_1(H)$, the curve $g(H)$ acquires a new maximum whose position in terms of the field H_n is practically independent of the plate thickness. In the region $\beta \ll 1$, the positions of the two maxima are determined by the equations

$$H_{GK} = 0.336 (2\pi b d^2 / l_0 u_L)^{1/2} (1 + 3.12\beta) H_L = 0.336 d (4\pi H_L^3 / l_0 d \Delta H)^{1/2} (1 + 3.12 l_0 / \pi d), \quad (33)$$

$$H_n = (2\pi b d^2 / l_0 u_L)^{1/2} (7^{1/2} - 1)^{-1} 3H_L \beta = (l_0 H_L^3 / \Delta H d)^{1/2} (7^{1/2} - 1)^{-1} 6\pi^{-1/2}. \quad (34)$$

Curves 2 and 3 of Fig. 1 show plots of the functions $(\beta x_{GK})^{-1}$ and $(\beta x_m)^{-1}$ as functions of β^{-1} . The maximum that varies with the maximum of $R_1(H)$, first increases with increasing d at $\beta \gg 1$ like $d^{1/4}$, and then decreases in the region $\beta \ll 1$ in proportion to d^{-1} . The new maximum, however, decreases like $d^{-1/2}$. Starting with $\beta = 0.06$, the new maximum becomes relatively higher. Curves 4 and 5 of Fig. 1 show the values of both maxima. The evolution of the function $e^{s/1} g(H)$ with changing thickness d is illustrated in Fig. 2, which shows a set of curves corresponding to different thicknesses at a fixed mean free path l_0 .

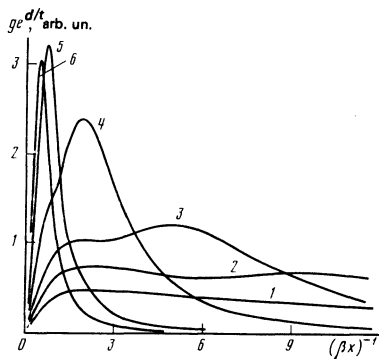


FIG. 2. Shapes of GKO envelopes. Curves 1–6 correspond to $\beta = 0.02, 0.05, 0.1, 0.3, 1.5,$ and 3 .

3. We proceed now to discuss the difference between the GKO in the two circular polarizations. It was shown earlier^{7,8} that in the case of specular reflection the GKO amplitudes are the same for the different polarizations. In strong fields, when $\xi_0 \ll 1$, these amplitudes coincide also in the case of diffuse reflection.² A difference between the GKO oscillations in circular polarizations was experimentally observed in Ref. 2. Mukhtarov and Gorshkov⁹ calculated the ratio $g_{sp}^{(+)} / g_{sp}^{(-)}$ and showed that the statement that the GKO amplitudes coincide in plus and minus polarizations is not quite exact. Namely, the ratio of these amplitudes reaches a minimum at $L\xi_0^2 \approx 1$, and differs from unity by an amount of the order of ξ_0 . This difference is actually insignificant. To observe the oscillations it is necessary to satisfy the inequality $L \gg 1$. Therefore $\xi_0 \ll 1$ in the region $L\xi_0^2 \sim 1$. In addition, in this field region the amplitudes of the doppleron oscillations and of the GKO are comparable, and the phases are indistinguishable, so that the difference between the GKO amplitudes is observable.

In diffuse scattering of the carriers there is another cause of the difference between the GKO amplitudes in the circular polarizations.¹ In this case the different components of the radio-frequency field influence one another and their amplitudes are interrelated. In the strong-field region $\xi_0 \ll 1$ the principal field components that determine the skin effect are the skin component and the GKC, and the amplitudes of the skin components are practically equal in the two polarizations. As a result, the GKO amplitudes are also equal. In the weak field region $\xi_0 \gg 1$, the principal components are a damped helicon at plus polarization and a quasihelicon at minus polarization. Their amplitudes are equal, and again the GKO amplitude is independent of the sign of the circular polarization. In intermediate fields, the doppleron amplitude becomes appreciable. In the vicinity of the doppleron threshold, where the wavelength of the skin component and of the doppleron turn out to be close and they interact resonantly, the doppleron amplitude has a maximum. It is precisely in this region that it is natural to expect the large difference between the GKO amplitudes in the circular polarizations. The amplitudes can differ not merely by several dozen percent, as in the field region $L\xi_0^2 \sim 1$, but by several times. The minimum value of the ratio $|g^{(+)} / g^{(-)}|$ depends on the mean free path l_0 . Under real conditions,

it depends also on the details of the FS and of the total damping of the doppleron.

2. EXPERIMENT

1. In the experiment we investigated the impedance of single-crystal tungsten and molybdenum plates in a magnetic field produced by a superconducting solenoid. The field was oriented along the [100] axis, whose direction was normal to the plate within 2° . The tungsten (molybdenum) samples were cut by the electric-spark method from stock pieces with relative resistivities $\rho_{300\text{K}} / \rho_{4\text{K}} = 50\,000$ and $35\,000$ (50 000); the plate surfaces were finished by the method described by Boiko and Gasparov.¹⁰ The ranges of the tungsten and molybdenum plate thicknesses were 0.09 – 2.89 and 0.47 – 1.83 mm. The samples were disks of diameter 7 and 4 mm in the case of tungsten and 3.5 mm in the case of molybdenum.

The measurements were made in a circularly polarized radio-frequency field in the temperature interval 1.5 – 5 K. The real and imaginary parts of the impedance were measured with an amplitude bridge and an autodyne.¹¹ The impedance oscillations ΔZ were recorded by separating the signal V_2 at double the magnetic-field modulation frequency. In the case of harmonic oscillations $V_2 \propto \Delta Z J_2(2\pi h / \Delta H)$, where J_2 is a Bessel function, h is the modulation amplitude, and ΔH is the period of the oscillations. The value of h was chosen to satisfy the condition $2\pi h / \Delta H \approx 3.1$, which corresponds to the first maximum of the function J_2 . This has made it possible to decrease considerably the measurement error due to the instability of the field h , as well as to facilitate the comparison of the amplitudes of the oscillations in samples of different thickness. The principal results were obtained at 500 kHz in one and the same pair of crossed coils of dimension such that the filling factor in all cases did not exceed 10% . It should be noted that measurement of the impedance of thick samples encounters experimental difficulties. The field-distribution inhomogeneity due to a sample thickness comparable with the diameter, as well as the presence of a large lateral surface, cause the registered signal to differ from the impedance Z_i of an infinite plate. Thus, at $H = 11$ kOe the ratios $R(d) / R_i$ at $d = 1.3$ and 2.89 mm are respectively 1.2 and 1.8 and decrease with increasing field, approaching unity in fields $H > H_m$. The oscillating part of the impedance is similarly distorted.

2. We consider now the results of the measurements of the smooth parts of the surface impedance of the tungsten samples in a magnetic field. The R_\pm curves reach a maximum at a certain field H_m whose value depends on the plate thickness. The measured values of $H_m(d)$ are shown in Fig. 3. It follows from the data of Fig. 3 that the $H_m(d)$ dependence is not linear, as it might be in the case of the normal skin effect in a magnetic field.³ The values of H_m for thick samples decrease noticeably with decreasing temperature. For the thinnest samples, both the shape of the $R(H)$ curves in fields $H < H_m(d)$ and the position of the $R(H)$ maximum are practically independent of temperature in the inter-

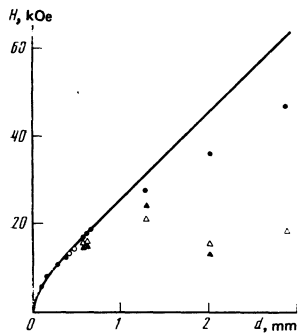


FIG. 3. Dependence of the values of H_m and H_{GK} on the plate thickness: ●) H_m for samples with resistivity ratio $\rho_{300K}/\rho_{4K} = 50\,000$; ○) H_m for samples with $\rho_{300K}/\rho_{4K} = 35\,000$; Δ) measured values of H_{GK} ; ▲) calculated H_{GK} ($l_0 = 1$ mm); curve—result of calculation of H_m ($l_0 = 1$ mm). (At $d < 0.5$ the values of H_{GK} are indistinguishable from H_m and are therefore not shown).

val 1.5–5 K.

Figure 4 shows plots of the ΔR_{\pm} oscillations of a tungsten plate 0.58 mm thick for the two circular polarizations of a radio-frequency field. The oscillations in the minus polarization are due to the propagation of the GKC, while in plus polarization they are superpositions of GKO and doppleron oscillations.¹² All these oscillations are connected with the DSCR of the holes of the octahedron located in the second Brillouin zone. It is seen that in both polarizations they are of comparable amplitude. (It must be borne in mind that in thin samples the doppleron oscillations are not harmonic near the threshold, so that their envelope can be distorted.) For thicker samples, the GKO are correspondingly decreased. This is illustrated by curves 1 and 2 of Fig. 5, which are the envelopes of the plots of ΔR_{\pm} for a

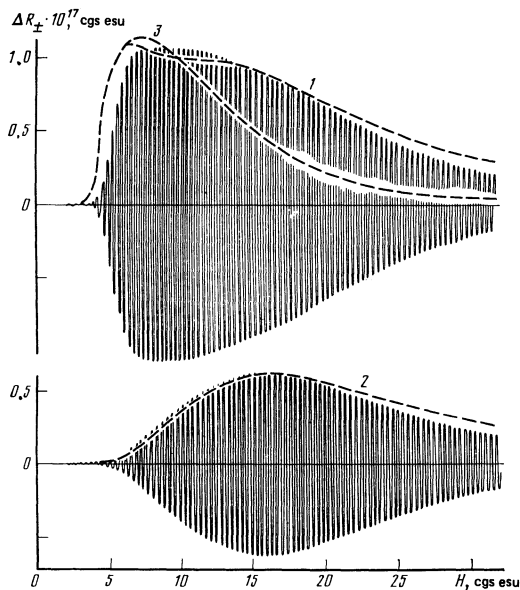


FIG. 4. Oscillations of ΔR_{\pm} in tungsten ($d = 0.58$ mm; $T = 4.2$ K; $f = 500$ kHz). Curves 1–3) result of calculation of the amplitudes of the oscillations of ΔR_{+} , ΔR_{-} , and the doppleron oscillations, respectively.

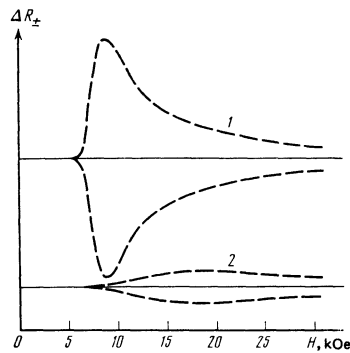


FIG. 5. Experimental envelopes of the oscillations of ΔR_{+} (curve 1) and ΔR_{-} (curve 2) for a tungsten sample with $d = 2.89$ mm; $T = 4.2$ K; $f = 500$ kHz.

plate 2.89 mm thick. In the region of the maximum of the envelope, the ΔR_{+} oscillations are due mainly to the doppleron. It is seen that the identification of the oscillation in tungsten, as well as in other metals, entails no great difficulty.

The period of the oscillations in strong magnetic fields is inversely proportional, in both polarizations, to the sample thickness and amounts to 71 Oe at $d = 2.89$ mm. From the measurement data for the holes of the octahedron we obtain the value

$$(\partial S/\partial p_z)_{\max} = (ed/c)\Delta H = 3.13\hbar\lambda^{-1},$$

which agrees with the results of Ref. 12. The product $\Delta H d$ for tungsten is equal to 20.5 Oe·cm. The field value $H_L^e = 3.1$ kOe at $f = 500$ kHz was determined from the plots of ΔR_{\pm} in the thinnest samples, where the true doppleron threshold is least masked by its damping.

In weak magnetic fields, ($H < H_L$), oscillations are observed on the $\Delta R_{\pm}(H)$ curves, with a period close to the period of the GKO in strong fields. They are, however, of relatively small amplitude and are hardly distinguishable on the curves of Fig. 4. Figure 6 shows plots of $\Delta R_{\pm}(H)$ in the weak-field region, obtained at a large gain. It is seen that the oscillations in the minus polarization are several times larger than in the plus polarization.

According to Figs. 4 and 5, the GKO amplitude has a

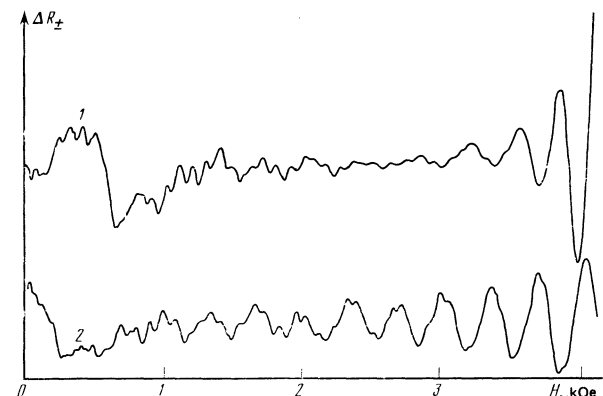


FIG. 6. Oscillations of ΔR_{+} and ΔR_{-} (curves 1 and 2) in tungsten ($d = 0.61$ mm; $T = 4.2$ K; $f = 500$ kHz).

maximum at a certain value of the field H_{GK} . For most samples, H_{GK} turns out to be close to the value of the field H_m and increases together with H_m with increasing d (see Fig. 3). For thick samples ($d=2.08$ and 2.89 mm), the growth of H_{GK} is no longer monotonic. Despite the large thickness difference, the values of the field H_{GK} for thick samples turn out to be close and much smaller than $H_m(d)$. Moreover, the values of H_{GK} for these two samples are less than for H_{GK} for a plate 1.3 mm thick.

For a subsequent comparison with the theory it is advantageous to obtain from the measurement data plots of $g^{(-)}/|Z_1^{(-)}|^2$ against the magnetic field, which characterize the behavior of the function $Hg_{sp}(H)$ (see Eq. (15)). The corresponding plots are shown in Fig. 7 in a log-log scale. The arrows on the figure mark the value of the field H_{GK} ; the thin vertical segments are the fields values for which $L\xi_0^2=0.2$. According to the theory,^{2,5} in the field region $L\xi_0^2 \ll 1$ the function $Hg_{sp}(H)$ should vary like $H^{-2.5}$ (the dashed line of Fig. 7). The observed difference between the experimental relations and the $H^{-2.5}$ law can be explained in the following manner. In the region $L\xi_0^2 > 0.2$ the experimentally determined exponent α is smaller than 2.5 because the parameter $L\xi_0^2$ is not small enough. In strong fields, the exponent α increases monotonically and exceeds 2.5 . The additional decrease of the GKO amplitude in strong fields can be due to the imperfection of the sample, namely to its deviation from plane-parallelism and its surface roughness. With increasing field, these factors should exert an ever more noticeable influence, since the displacement of the carriers in strong fields becomes commensurate with the parameters that characterize the imperfection of the plate. For not too thin samples, in fields $H \approx H_{\text{GK}}$, the function $g^{(-)}/|Z_1^{(-)}|^2$ varies approximately like $H^{-2.7}$.

At the chosen plate preparation method, the values of α in identical magnetic fields $L\xi_0^2 \ll 1$ differ insignificantly. It was therefore possible to determine, from

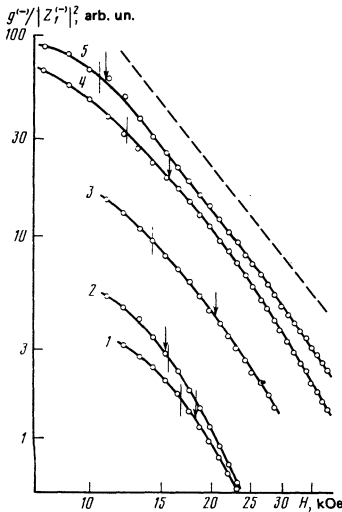


FIG. 7. Dependence of $g^{(-)}/|Z_1^{(-)}|^2$ on the magnetic field. Curves 1–5 correspond to samples with $d=2.89, 2.03, 1.30, 0.58,$ and 0.28 mm.

the measured GKO amplitude and from the smooth parts of the impedance of plates with different thicknesses in fields $L\xi_0^2 \ll 1$, the mean free path l of the resonant carriers under the assumption that it is the same for all the samples cut from the same ingot. The value of l is given by

$$l = (d_1 - d_2) \ln [A_2 d_2^{\eta} |Z_1^{(1)}|^2 / A_1 d_1^{\eta} |Z_1^{(2)}|^2], \quad (35)$$

where A_1 and A_2 and $Z_1^{(1)}$ and $Z_1^{(2)}$ are respectively the GKL amplitudes and the smooth parts of the impedance in the minus polarization in samples of thickness d_1 and d_2 . All the quantities must be obtained at the same value of the magnetic field. The accuracy is higher the greater the difference between d_1 and d_2 . According to the measurement data obtained for different pairs of samples, $l = 1 \pm 0.2$ mm.

The path length l can in principle be determined from the doppleron oscillations. In a strong field ($\xi_0 \ll 1$) their amplitude is proportional to $|Z_1^{(+)}|^2 \exp(-d/l)$. Unfortunately, in this field region the doppleron-oscillation and GKO amplitudes are comparable, so that it is difficult to discern the doppleron contribution on the ΔR_s plots. The value of l is difficult to distinguish on ΔR_s plots also in a weaker field (where the GKO are small), because of the already mentioned anharmonicity of the oscillations. A more correct value of l could be determined from the doppleron oscillations in $R_s(H)$ in weak field. The corresponding calculation of the mean free path in fields $H_L < H < 1.5 H_L$ yields values $l = 0.4-0.7$ mm, while measurements in a stronger field give larger values of l . This means that in the considered field region the doppleron damping length is less than the resonant-hole mean free path.

We shall be interested hereafter also in the mean free path l_0 averaged over the FS. It can be estimated from the static resistance and from the data, e.g., of Ref. 13. This estimate yields a value $l_0^e = 1.2-1.3$ mm at $T = 4.2$ K.

3. DISCUSSION OF RESULTS

1. We shall compare, for the sake of argument, the theory with the experimental data obtained at $T=4.2$ K and $f=500$ kHz. It is necessary to substitute in the equations of Sec. 1 the parameters $(\partial S/\partial p_x)_{\text{max}}, H_L, \gamma = u/2\pi l, \gamma_1 = u/\pi l_0 - \gamma$, which must be reconciled with the experimental conditions, and carry out a numerical calculation. In the preceding section we obtained $(\partial S/\partial p_x)_{\text{max}} = 3.13 \text{ \AA}^{-1}$ and $l=1$ mm.

The skin component of the field and the short-wave components connected with the DSCR depend, generally speaking on the different collision frequencies of the holes and electrons. In our model, however, the hole scattering is described by a single parameter γ . This shortcoming can be eliminated by choosing the parameter γ_1 to agree with the mean free path l_0 and by not assuming it to determine the frequency of the electron collision. We put tentatively $l_0 = l = 1$ mm.

In the theory, the threshold field H_L must not necessarily coincide with the experimental H_L^e . The point is that our FS model describes correctly the resonant sin-

gularity of the nonlocal conductivity, but not its value far from resonance, since it does not take into account the details of the real FS. We are therefore justified in claiming quantitative agreement with experiment in strong fields, but can count only on a qualitative agreement in weak fields in the vicinity of the doppleron threshold. To determine the parameter H_L we use the $H_m(d)$ plot of Fig. 3. According to (28), the value of H_m in the case $l_0 \gg d$ is determined by the value of H_L and is practically independent of l_0 . It turns out that it is possible to choose a value $H_L = 3.15$ kOe such that the theoretical curve $H_m(d)$ (solid line in Fig. 3) passes near the experimental points that pertain to thin samples. This is evidence that for thin samples there is realized the nonlocal effect of Fisher and Kao. This is confirmed also by the fact that H_m of the thinnest samples is independent of the temperature and of the residual resistivity. The proximity of the theoretical value of H_L to the experimental $H_L^e = 3.1$ kOe shows that our model describes correctly the nonlocal conductivity far from resonance, too.

It is seen from Fig. 3 that with increasing H the theoretical curve deviates noticeably from the experimental points. We did not determine exactly the value of the parameter l_0 in our analysis. By choosing this parameter it would be possible to obtain better agreement between theory and experiment for $H_m(d)$ also in the region of large d (without disturbing the agreement for small d). The value of l_0 can be approximately obtained, e.g., from the slope of the line drawn through the experimental $H_m(d)$ points for thick samples, or from its intercept on the ordinate axis [see Eqs. (29) and (30) as well as Fig. 3]. In this case, however, l_0 turns out to be too large (3 mm), greatly exceeding the value $l_0^e = 1.3$ mm estimated from the static resistance. Since l_0 determines also the static magnetoresistance, it must not exceed l_0^e . The discrepancy between theory and experiment at large H is apparently due to the fact that thick samples can not be regarded as plates. One can attempt to determine l_0 from the behavior of the quantity $X_1/(R_1 - X_1)$ in the field region $H_L < H < H_m$ [see Eqs. (16) and (17)]. Unfortunately, this method yields values of l_0 scattered in the interval 0.6–2.5 mm.

2. We discuss now the behavior of the maximum of the GKO amplitude. In accordance with the theory, the maximum-amplitude field H_{GK} in thin samples is in the vicinity of the field H_m . In thick samples $d = 2.03$ and 2.89 mm, the fields H_{GK} turn out to be much weaker than $H_m(d)$ and differ little from each other. This is evidence that in thick samples there appears the new GKO-amplitude maximum described in the theory. Unfortunately, a direct quantitative comparison of the results of the theory and of the experiment is impossible. Owing to the imperfection of the samples, in a strong field the quantity $g/|Z_1^{(-)}|^2$ decreases in proportion to α raised to a power higher than the theoretical 2.5, and this power increases with H (see Fig. 7). As a result, the position of the new maximum H_n may not coincide with the calculated one, and the second maximum, which is close in position to H_m , which remains in the theory, is not observed in experiment because of the strong increase of α . (In the field region $q_1 < \xi_0$, in

which the maximum of the GKO amplitude is observed in thick samples, the factor R/R_n can be regarded as constant, so that we shall neglect its effect on H_n).

If the power 2.5, which determines the decrease of the function $Hg_{sp}(H)$, is replaced in the expressions of the theory by an arbitrary power α , then the position of the new maximum will be given by

$$H_n \approx (l_0 H_L^3 / \pi \Delta H d)^{1/\alpha} \cdot 2(4-\alpha) \{ [1 + (\alpha-2)(4-\alpha)]^{1/\alpha} + \alpha - 1 \}^{-1}, \quad 2 < \alpha < 4. \quad (36)$$

An important role is played by the value $\beta_0(\alpha)$ at which the new maximum for a given power of α first appears. For thick samples the values of α in the vicinity of the maximum of the GKO amplitude are $\alpha_{1,3} = 2.6 \pm 0.2$; $\alpha_{2,03} = 2.8 \pm 0.2$; $\alpha_{2,89} = 2.8 \pm 0.2$. The calculated values of $\beta_0(\alpha)$ in this α interval, as well as the value of $y_0(\alpha) = 1/\chi_H[\beta_0(\alpha)]$, are

| α | 2.5 | 2.6 | 2.7 | 2.8 | 2.9 | 3.0 |
|-------------------|-------|-------|-------|-------|-------|-------|
| $\beta_0(\alpha)$ | 0.10 | 0.13 | 0.16 | 0.19 | 0.23 | 0.27 |
| $y_0(\alpha)$ | 0.165 | 0.179 | 0.185 | 0.180 | 0.185 | 0.181 |

From the condition that the new maximum appear already for the samples with $d = 2.03$ and 2.89 mm, it is possible to estimate from $\alpha_{2,03}$ and $\alpha_{2,89}$ that the average mean free path $l_0 < 1.3$ mm. Therefore the old maximum is still observed in a sample with $d = 1.3$ mm, and with the aid of $\alpha_{1,3}$, we obtain the lower-bound estimate $l_0 < 0.5$ mm. The upper-bound estimate can be refined. Using the approximate constancy of $y_0(\alpha)$ in the given α interval, we can write down for the samples in which the new maximum is observed the inequality

$$y = (l_0 \Delta H d / 4\pi d^2 H_L^3)^{1/\alpha} H_n < y_0.$$

Substitution of the numerical values yields $l_0 < 1.1$ mm. The error in α does not make it possible to determine l_0 more accurately also from the value of H_n [see Eq. (36)]. We assume $l_0 = 1$ mm. Figure 3 shows the calculated values of the field of the GKO maximum. It is seen that they are in fair agreement with experiment.

The value of β for our samples ranges from 3 to 0.1. The change of the maximum of the GKO amplitude, multiplied by $e^{d/l}$, with increasing d is small and agrees with the character of curve 5 on Fig. 1.

Knowing the values of $l_0, l, H_L, (\partial S / \partial p_x)_{min}$, we can calculate completely the plate impedance in both strong and weak magnetic fields. The calculated behavior of the smooth part of the impedance as a function of the magnetic field, in the case of samples that are not very thick, agrees well with experiment. The theoretical maximum of R agrees approximately within 5% with experiment. The calculated behavior of the amplitude of the oscillations with changing magnetic field, in both polarizations, for samples with $d < 0.61$ mm, agrees well with experiment. The calculated results for $d = 0.58$ mm are shown by the dashed curves in Fig. 4 (curve 3 represents the doppleron oscillations). Only near the strongest fields do the oscillations in the experiment decrease markedly more rapidly than in experiment, owing to imperfection of the samples.

The absolute values of the oscillation amplitudes differ systematically in theory and experiment. For $d = 0.28$ mm they are 2.5 times larger than in experiment in the field interval 9–22 kOe. At $d = 0.58$ mm, this

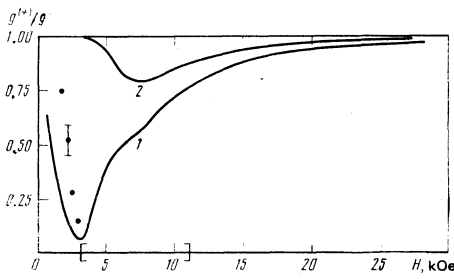


FIG. 8. Ratio of the GKO amplitudes in plus and minus polarizations: 1) calculation for specularity coefficient $p = 0$; 2) calculation for $p = 1$; points—results of measurements on tungsten sample ($d = 0.61$ mm; $T = 4.2$ K; $f = 500$ kHz).

difference is 2.2. Accordingly, we chose for the calculated curves in Fig. 4 a scale smaller by a factor 2.2. The reason why the amplitudes differ is possibly that the carrier reflection from the plate surface in tungsten is not completely diffuse.

We note that according to theory the maximum GKO amplitude in pure diffuse reflection is much larger than in specular reflection. Thus, for $d = 0.58$ mm the ratio of the amplitude is 370. There is therefore puzzling why it is concluded in Ref. 14 that the oscillations depend little on the character of the reflection and that the results of measurements on tungsten are comparable with theory for pure specular reflection.

3. Finally, we examine in greater detail the GKO in weak fields. Figure 8 shows the calculated plot of the ratio of the GKO amplitudes in plus and minus polarizations. The square brackets on the abscissa axis mark the field region where the amplitude of the doppleron oscillations exceeds the GKO amplitude and no different between the GKO in different polarizations is observable. The same figure shows points corresponding to the ratio of the GKO amplitudes as obtained from experiment. The vertical segment indicates the measurement error due to the difficulty in determining the amplitudes of the investigated GKO, which are observed in weak fields against a background of oscillations having different periods (see Fig. 6). It follows from an examination of Fig. 8 that experiment and theory are in qualitative agreement. For comparison, the same figure shows curve 2, which represents the analogous ratio for the case of pure specular reflection. Thus, the noted deviation of the character of the reflection from specularity causes the GKO in the vicinity of the doppleron threshold to be substantially lower in its polarization than in the opposite polarization. It appears that a similar situation obtains in cadmium below the hole-doppleron threshold.²

We have compared above the conclusions of the theory with the measured impedances of tungsten samples. The results of the experiments with molybdenum reveal the same regularities as for tungsten.

The authors are deeply grateful to V. A. Gasparov for helpful discussions and for supplying the samples.

APPENDIX

According to Ref. 1, the quantities Z_∞ , I , and g_{sp} ,

which enter in the expression for the plate impedance, are given by

$$\frac{4\pi q_0}{cZ_\infty} = \frac{i}{2\pi} \int_{-\infty}^{\infty} dq \ln \frac{D(q)}{q^2}, \quad (\text{A.1})$$

$$I(q) = \frac{i}{2\pi} \int_{C_1} dz \frac{D'(z)}{D(z)} \ln(z-q), \quad (\text{A.2})$$

$$g_{sp}(L) = \frac{1}{\pi i} \int_{C_1} \frac{dq}{D(q)} e^{iqL}, \quad (\text{A.3})$$

where $D'(z)$ is the derivative of $D(z)$, the contour C_2 encircles clockwise the cut drawn from the point $-\Gamma$ to ∞ , and the contour C_1 encircles counterclockwise the cut drawn from the point Γ to $-\infty$.

Integrating the right-hand side of (A.1) by parts and deforming the integration contour to the contour C_2 , we obtain

$$\frac{4\pi q_0}{cZ_\infty} = q_1 + q_2 + \frac{1}{2\pi i} \int_{C_2} \left[\frac{D'(q)}{D(q)} - \frac{2}{q} \right] q dq, \quad (\text{A.4})$$

where account was taken of the contributions of the two poles of the function D'/D at the points $q = -q_1$ and $q = -q_2$. The second term in the brackets can be left out, since it has no branch points.

We represent the function D in the form $D = A - B$, where A is the rational part of D , and B contains the square root. It is convenient to represent the integral in (A.4) in the form

$$\frac{1}{2\pi i} \int_{C_2} \frac{D'(q)}{D(q)} q dq = \frac{1}{2\pi i} \int_{C_2} \left(\frac{AA' - BB'}{A^2 - B^2} + \frac{A'B - AB'}{A^2 - B^2} \right) q dq. \quad (\text{A.5})$$

The first term in the parentheses has a simple pole at the point $q = -\Gamma$ ($B \rightarrow \infty$ at this point), and its integral is equal to $-\Gamma/2$. The integral of the second term, which has a branch point, will be calculated by the method described in Ref. 4. This integral does not change if the integrand is multiplied by the function $(2/\pi)\arcsin(-q/\Gamma)$. Since the integrand is odd, the integral along the contour C_2 is equal to half the integral over the closed contour C_3 , made up of the contour C_2 , the contour C_1 traced in the opposite direction, and two infinite semi-circles. The integrand has inside this contour only simple poles at the points $\pm q_1, \pm q_2, \pm q_3$. Recognizing that $B = A$ for the roots of the dispersion equation that are located on the first sheet, and $B = -A$ for the roots on the second sheet, we find that the integral of the second term in the parentheses of (A.5) is

$$-\frac{1}{\pi} \left[q_1 \arcsin \frac{q_1}{\Gamma} + q_2 \arcsin \frac{q_2}{\Gamma} - q_3 \arcsin \frac{q_3}{\Gamma} \right]. \quad (\text{A.6})$$

Adding to this the previously obtained term, we arrive at Eq. (10).

We now transform the integral (A.2). We note first that

$$\frac{i}{2\pi} \int_{C_1} \frac{D'(z)}{D(z)} dz = -2. \quad (\text{A.7})$$

To prove this, we subtract from the integrand the quantity $2/z$, the integral of which along the contour C_2 is zero, and taking into account the fact that the integral of the obtained function is equal to half the integral over

the contour C_3 . The latter is equal to the number of roots of the dispersion equation on the first sheet, taken with opposite sign.

If we now use (A.7), take the residue to the integrand in (A.2) at the pole located at the point $z = -\Gamma$, reduce the integrals along the edges of the cut to a single integral, and make the substitution $z = -\Gamma x$, then the expression for $I(q)$ takes the form

$$I(q) = -\frac{1}{2} \ln \left(1 + \frac{q}{\Gamma} \right) + \frac{\xi}{\pi} \int_1^{\infty} \frac{(3x^2 - 2 - \xi) \ln(x + q\Gamma^{-1})}{(x^2 - \xi)^2 (x^2 - 1) + \xi^2} \frac{dx}{(x^2 - 1)^{3/2}}. \quad (\text{A.8})$$

Making the change of variable $x = (z^2 + 1)^{1/2}$, we arrive at expression (12), which is more convenient for calculations.

Finally, to obtain (13) it is necessary to substitute the function $D(q)$ in (A.3), reduce the integral along the edges of the cut to a single integral, and to make the same variable changes as before.

¹⁾ Unfortunately, the upper integration limit was not printed in the two basic integro-differential equations solved in Ref. 1. It should be ∞ in (1) and equal to L in (23).

¹I. F. Voloshin, V. G. Skobov, L. M. Fisher, and A. S. Chernov, Zh. Eksp. Teor. Fiz. **80**, 183 (1981) [Sov. Phys. JETP **53**, 92 (1981)].

- ²I. F. Voloshin, V. G. Skobov, L. M. Fisher, and A. S. Chernov, *ibid.* **72**, 735 (1977) [**45**, 385 (1977)].
- ³Harris Fisher and Yi-Han Kao, Sol. State Comm. **7**, 275 (1960).
- ⁴D. É. Zherebchevskii and V. P. Naberezhnykh, Fiz. Nizk. Temp. **4**, 467 (1978) [Sov. J. Low Temp. Phys. **4**, 229 (1978)].
- ⁵I. F. Voloshin, V. G. Skobov, L. M. Fisher and A. S. Chernov, Zh. Eksp. Teor. Fiz. **78**, 339 (1980) [Sov. Phys. JETP **51**, 170 (1980)].
- ⁶D. E. Zherebchevskii, V. I. Naberezhnykh, and V. V. Chabachenko, Fiz. Nisk. Temp. **6**, 382 (1980) [Sov. J. Low Temp. Phys. **6**, 428 (1980)].
- ⁷V. F. Gantmakher and É. A. Kaner, Zh. Eksp. Teor. Fiz. **48**, 1572 (1965) [Sov. Phys. JETP **21**, 1053 (1965)].
- ⁸D. S. Falk, S. Gerson, and J. F. Carolan, Phys. Rev. **B1**, 407 (1970).
- ⁹M. A. Mukhtarov and V. N. Gorshkov, Zh. Eksp. Teor. Fiz. **75**, 291 (1978) [Sov. Phys. JETP **48**, 145 (1975)].
- ¹⁰V. V. Boiko and V. A. Gasparov, *ibid.* **61**, 2362 (1971) [**34**, 1266 (1972)].
- ¹¹I. F. Voloshin, V. G. Skobov, L. M. Fisher, Z. S. Chernov, and V. A. Yudin, *ibid.* **73**, 1884 (1973) [**46**, 989 (1977)].
- ¹²I. M. Vitebskii, V. T. Vichinkin, A. A. Galkin, Yu. A. Ostroukhov, O. A. Panchenko, L. T. Tsymbal and A. N. Cherkasov, Fiz. Nizk. Temp. **1**, 4001 (1975) [Sov. J. Low Temp. Phys. **1**, 2031 (1975)].
- ¹³V. I. Cherepanov, V. E. Startsev, and N. V. Volkenshtein, *ibid.* **6**, 890 (1980) [**6**, 432 (1980)].
- ¹⁴O. A. Panchenko, V. V. Vladimirov, P. P. Lutsishin, and M. A. Mukhtarov, Zh. Eksp. Teor. Fiz. **74**, 658 (1978) [Sov. Phys. JETP **47**, 346 (1978)].

Translated by J. G. Adashko